

Advanced Cooled Turbine Airfoil Aerodynamic Investigation

W. G. Hess*

Pratt & Whitney Aircraft Group, West Palm Beach, Fla.

Several convectively cooled trailing-edge designs were investigated to eliminate the need for film cooling on the airfoil suction side. A first-stage turbine vane having potential application for an advanced Air Force fighter engine was selected for the evaluation. The final design eliminates film cooling on the suction side and uses the wavy crisscross slot as the trailing edge cooling scheme. The cooling design was incorporated into a cascade airfoil using the radial wafer fabrication technique and evaluated in an airfoil cascade test. The results are presented which indicate significant improvements in the aerodynamic and cooling performance.

Nomenclature

D	= diameter, in.
g	= units constant, $\text{lb}_m\text{-ft}/\text{lb}_f\text{-s}^2$
h	= enthalpy, Btu/lb_m
p	= pressure, $\text{lb}_f/\text{in.}^2$
T	= temperature, $^\circ\text{R}$
V	= velocity, ft/s
W	= flowrate, lb_m/s
γ	= specific heat ratio
ϕ	= cooling effectiveness
$(1 - \phi^2)$	= aerodynamic profile loss coefficient

Subscripts

a	= actual
C	= coolant
G	= gas
i	= isentropic process
o	= total
s	= static
W	= wall
1	= upstream position
2	= downstream position

I. Introduction

COOLING studies of advanced reduced solidity turbines indicate that in order to meet the increased heat loads, conventionally cooled trailing-edge designs must be augmented by film cooling to effectively lower the mainstream gas temperature adjacent to the walls. Unfortunately, use of film cooling, especially in the high Mach number regions of the airfoil, increases aerodynamic losses which are proportional to the Mach number squared. The high Mach numbers occur on the suction side of the airfoil in the region of the gage point downstream to the trailing edge. The trailing-edge region of turbine airfoils is difficult to cool because 1) the cooling air is hot when it arrives at the trailing edge, since it has been used to cool other portions of the airfoil, and 2) the trailing-edge thickness is relatively thin, and, in the past, has restricted convective cooling geometries to drilled passages or cast pedestals which are amenable to fabrication by conventional manufacturing methods. This problem is aggravated in reduced solidity designs with increased suction-side Mach number and long surface distance from gage point to trailing edge.

Presented as Paper 77-950 at the AIAA/SAE 13th Propulsion Conference, Orlando, Fla., July 11-13, 1977; submitted July 13, 1977; revision received May 11, 1978. Copyright © American Institute of Aeronautics and Astronautics, Inc., 1977. All rights reserved.

Index categories: Aerodynamics; Performance.

*Senior Engineer, Turbine Technology Group, System Design.

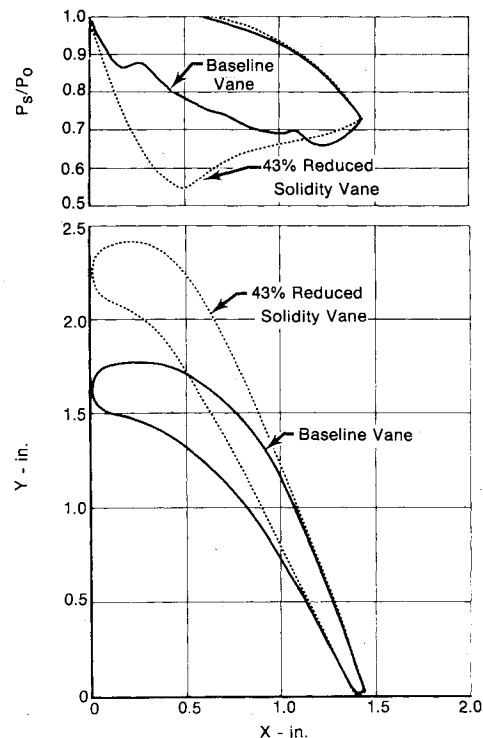


Fig. 1 Pressure profiles for conventional and 43% reduced solidity vanes.

The objective of this program was to demonstrate an improved low-solidity turbine airfoil design for advanced high-temperature turbines. Specifically, the program was aimed at demonstrating an airfoil design with improved convective cooling features in the trailing edge that minimize or negate film cooling on the suction side which is detrimental to aerodynamic performance. The aerodynamic performance goal of the 43% reduced solidity airfoil design was set equal to that obtained with the conventional solidity airfoil. The cooling goal was to obtain an airfoil that operated with a maximum wall temperature below the life requirement limit of 2000°F.

The program was divided into three separate tasks: task I consisted of studying various improved convective cooling schemes for the trailing edge, which eliminated the need for film cooling on the airfoil suction side; in task II, the best trailing-edge cooling scheme identified in task I was incorporated into a test airfoil, which was representative of an advanced reduced solidity turbine vane midsection having potential application for an advanced Air Force fighter engine; and subsequently, in task III, a cascade test was

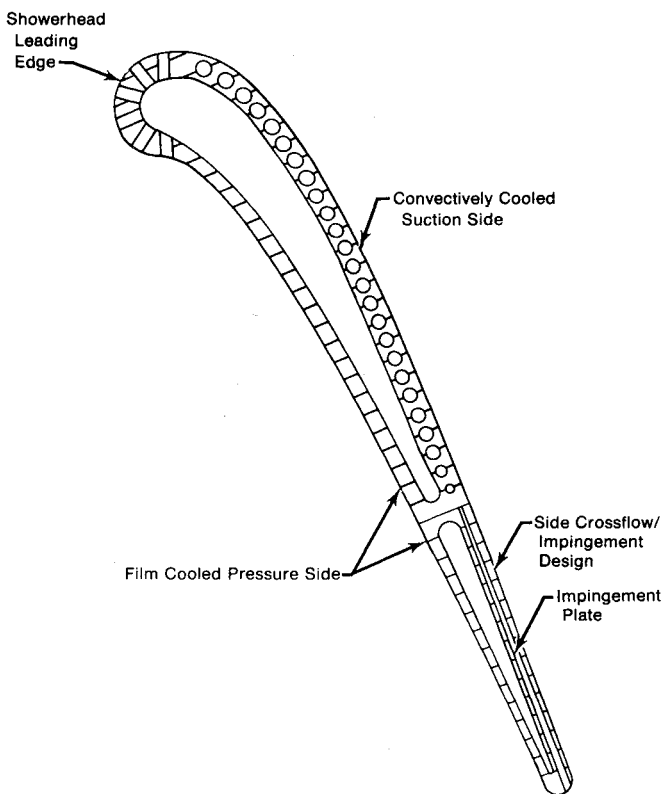


Fig. 2 43.4% reduced solidity airfoil crossflow/impingement design.

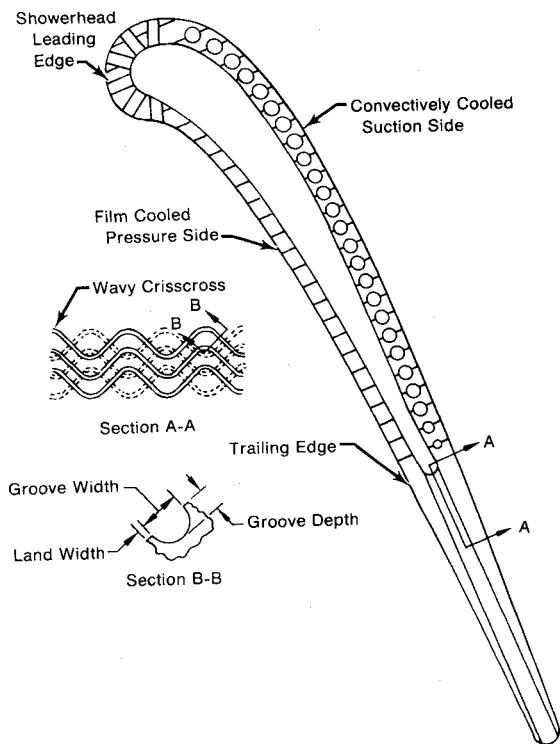


Fig. 3 Reduced solidity airfoil, wavy crisscross slot design.

conducted at reduced temperature and pressure to determine the aerodynamic and cooling performance of the cooling design.

II. Airfoil Design Study

The pressure profile and cross section for the 43.4% reduced solidity airfoil used in this program is presented in Fig. 1. The corresponding data for the conventional solidity

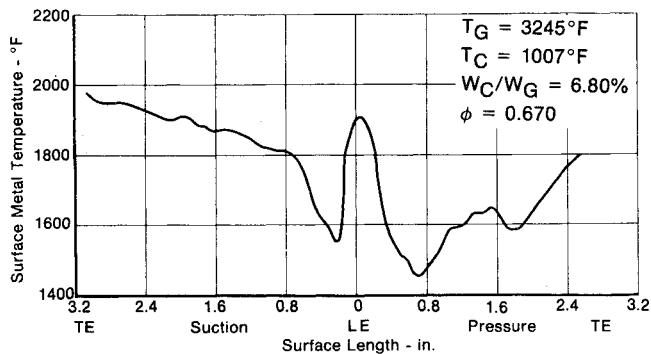


Fig. 4 Predicted metal temperature profile for the 43.4% reduced solidity radial wafer airfoil, wavy crisscross slot design.

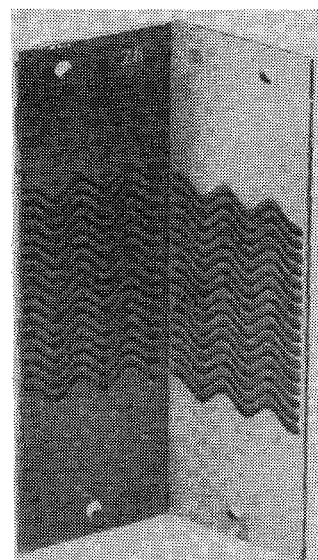


Fig. 5 Trailing-edge wafers with the wavy crisscross slot design for the 43.4% reduced solidity first-vane airfoil.

vane are included for comparison. The pressure profile data illustrate the low-suction side static pressures, i.e., high Mach numbers associated with the reduced solidity design, and the need to eliminate or minimize film cooling in that area.

Detailed heat transfer investigations were conducted on two candidate trailing-edge cooling designs, crossflow/impingement and the wavy crisscross slot, and on several modifications of each. The analysis included determining the external heat transfer coefficients; gas stream film temperatures; coolant flow distribution, heat transfer coefficients, and pressure losses; and airfoil wall temperatures. For the design phase, a hot-spot temperature limit of 2000°F was determined as the maximum allowable for the airfoil to meet the life requirements.

The final crossflow/impingement design investigated is shown in Fig. 2. It consists of a six-row showerhead, film cooling on the pressure side, radial cooling passages on the suction side, and the crossflow/impingement design in the trailing-edge section. The coolant in the radial passages discharges into the vane platform area and ultimately can be used to cool the blade rub strip or the platform since vane coolant can be supplied from either o.d. or i.d. The double use of this coolant is a potential means to increase the engine cycle efficiency by reducing the total amount of coolant required. For this design, the number of impingement holes in the beginning of the trailing-edge section and the discharge gap at the end of the trailing-edge section were both increased relative to the initial design to increase the coolant flow through the trailing edge. However, even with these modifications, the predicted wall temperature for the trailing-edge section exceeded the life requirement limit and this cooling scheme was eliminated from the design study.

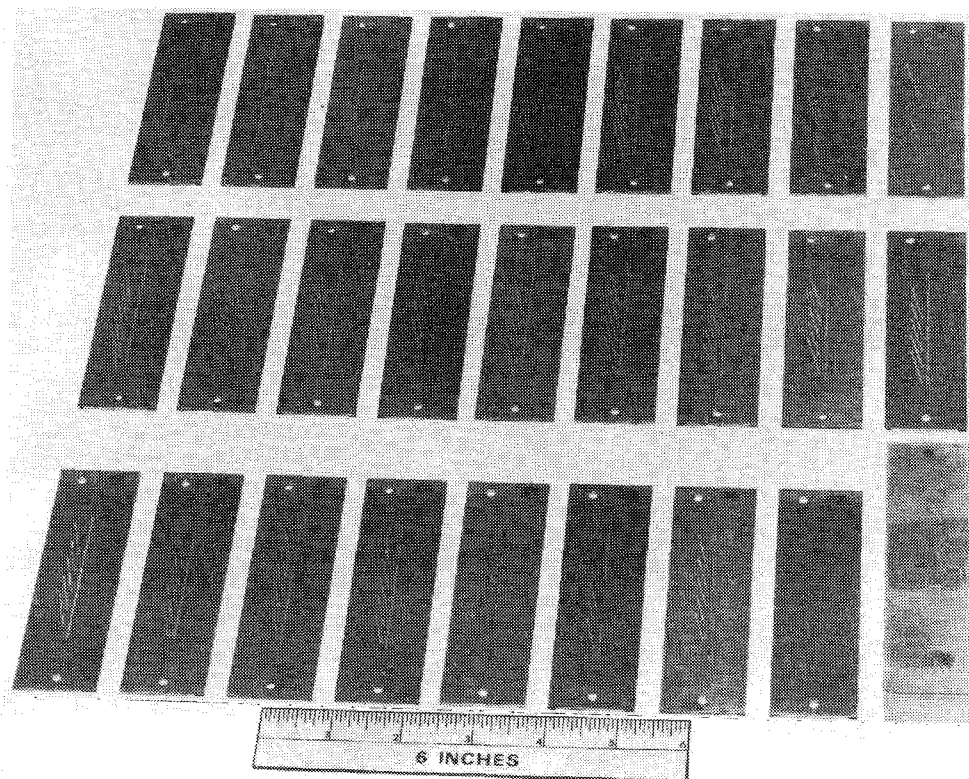


Fig. 6 First set of etched wafers and trailing-edge block for the 43.4% reduced solidity radial wafer airfoil.

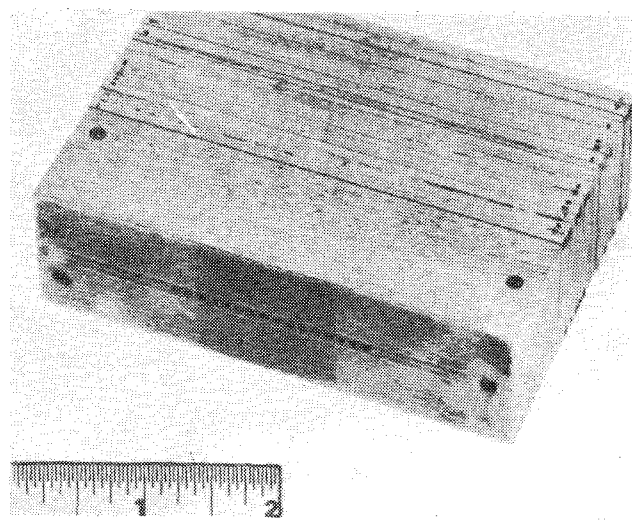


Fig. 7 Bonded wafers and trailing-edge block for the 43.4% reduced solidity radial wafer airfoil.

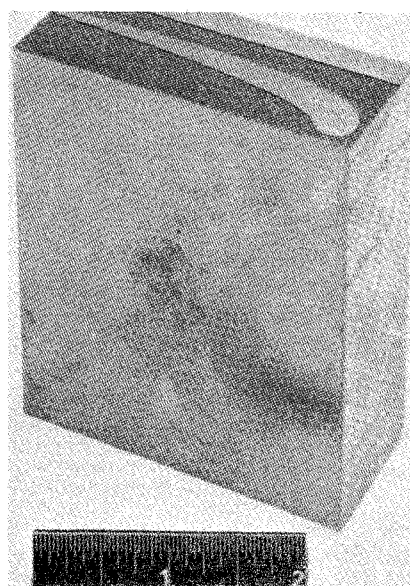


Fig. 8 Initial cascade airfoil machining from bonded block.

The final wavy crisscross slot design shown in Fig. 3 utilizes the same cooling design as the crossflow/impingement design for the front portion of the airfoil. For the trailing-edge section, however, the wavy crisscross slot design is employed. This design increases the passage turbulence by the two coolant paths turning and crossing one another. The predicted metal temperature profile for the final design is shown in Fig. 4. As indicated, the suction-side trailing-edge metal temperature is below the life requirement limit of 2000°F.

III. Airfoil Hardware Design and Fabrication

The cooling design was incorporated into a cascade test airfoil using the radial wafer fabrication technique. The airfoil is a constant cross section airfoil with a 3.0 in. span. The wafers which formed the trailing-edge cooling design of a wavy crisscross slot were fabricated first, since they were bonded in a subassembly and then bonded with the remaining wafers to form the block from which the cascade airfoil was

machined. A photograph of the trailing-edge wafers is presented in Fig. 5. The wafers were bonded together using a join-process called Transient Liquid Phase (TLP™)† bonding.

The cascade airfoil consists of 27 individual wafers and the trailing-edge block as shown in Fig. 6. The wafers and the trailing edge block were bonded together; a photograph of the block which formed the cascade airfoil is shown in Fig. 7. The initial electrical discharge machining (EDM) of the airfoil external contour from the bonded block is presented in Fig. 8. The airfoil shown in Fig. 9 was then obtained by machining the internal cavity, external contour, and showerhead holes.

†TLP bonding is a Pratt & Whitney Aircraft process for joining superalloys. The process achieves near-parent metal strength but requires only moderate bonding pressures of 15 to 20 psi, compared to conventional diffusion bonding pressures, which are generally in excess of 2000 psi.

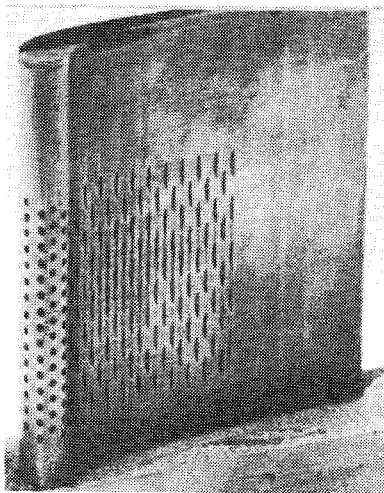


Fig. 9 43.4% reduced solidity radial wafer airfoil in holder for machining.

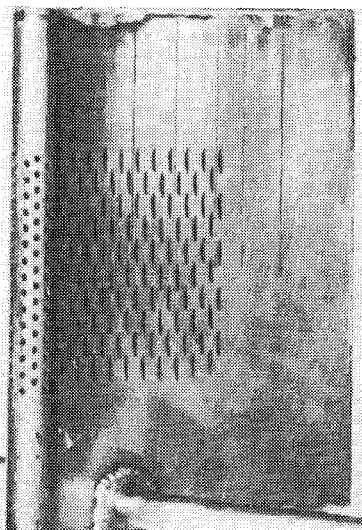


Fig. 10 43.4% reduced solidity radial wafer airfoil.

The final steps in the fabrication process were the machining of the thermocouple instrumentation slots and the addition of the coolant manifold and supply tubes. A photograph of the completed airfoil with the thermocouple instrumentation slots and the supply manifolds is presented in Fig. 10.

IV. Airfoil Cascade Test

Test Rig Description

Test facility air is provided by compressor bleed from a J75 slave engine (Fig. 11). The maximum airflow capacity is 28 lb/s. Inlet airflow is controlled by a 10 in. control valve and measured with a sharp-edged ASME standard orifice. Air temperature can be regulated from 160-600°F with a water-cooled heat exchanger located upstream of the test rig.

The airfoil performance test was conducted in the plane cascade rig shown in Fig. 12. Air is supplied to the test section through a 36-in.-diameter plenum chamber, which is equipped with static pressure ports and temperature probes for determining rig inlet conditions. The rig has a rectangular transition duct or channel designed to provide two-dimensional flow conditions at the inlet to the test airfoil pack. Air inlet angles to the airfoil pack can be varied from -10 to 65 deg. The channel width in the airfoil gapwise direction can be varied up to a maximum of 18 in.; the channel height in the airfoil spanwise direction is 3 in.

Test Airfoil Description

The cascade airfoil pack consisted of six constant cross section stainless steel slave airfoils and the radial wafer test

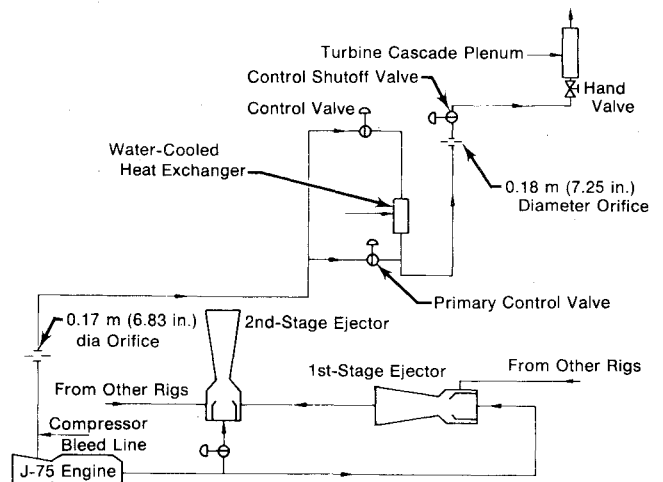


Fig. 11 Test facility air supply schematic.

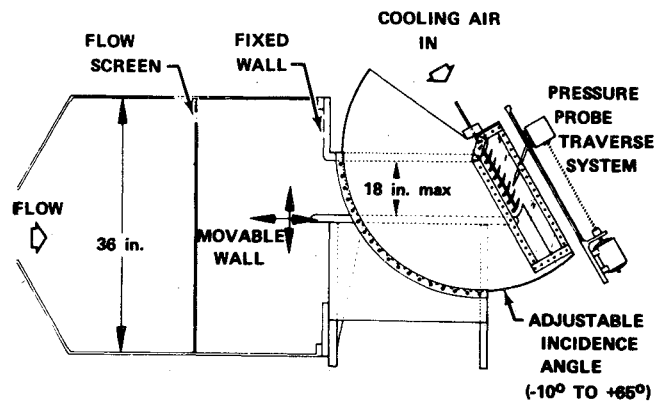


Fig. 12 Turbine plane cascade rig.

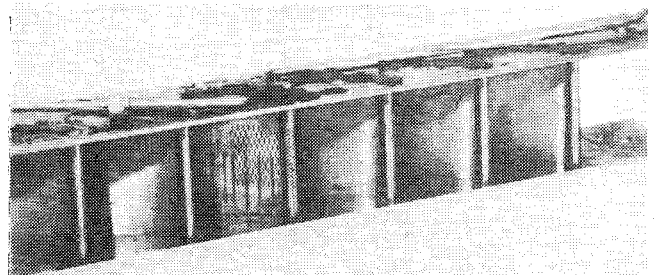


Fig. 13 Cascade assembly for the 43.4% reduced solidity radial wafer airfoil.

airfoil located in the center position. Photographs of the assembled airfoil pack and a closeup of the test airfoil are presented in Figs. 13 and 14, respectively. The test section passage height is 3 in.; however, only the middle 1.65 in. was cooled. This height corresponds to the exit span of a typical first-stage turbine vane. Two air lines were utilized to supply the coolant to the test airfoil. One line supplied coolant to a common plenum which fed the leading edge, pressure side, and trailing edge and the other line supplied coolant to the suction-side radial passages.

Instrumentation

In the plane cascade test, instrumentation was provided to measure airfoil pack total pressure losses, important inlet and exit mainstream flow conditions, coolant inlet flow conditions, and airfoil wall temperatures. The coolant inlet temperature and pressure to the test airfoil were determined for each of the supply lines. The airfoil was instrumented with

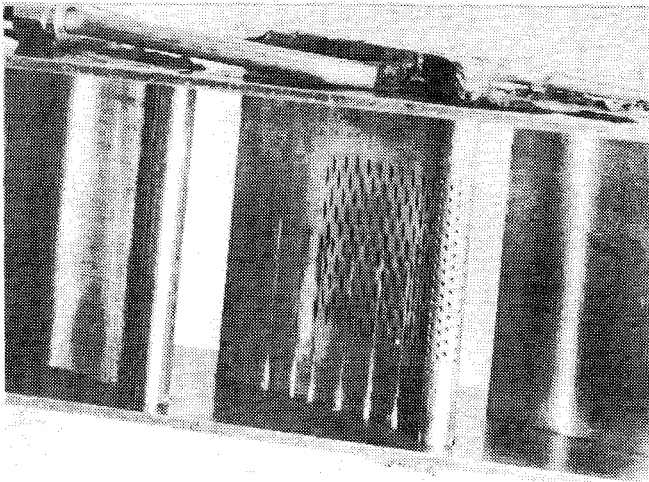
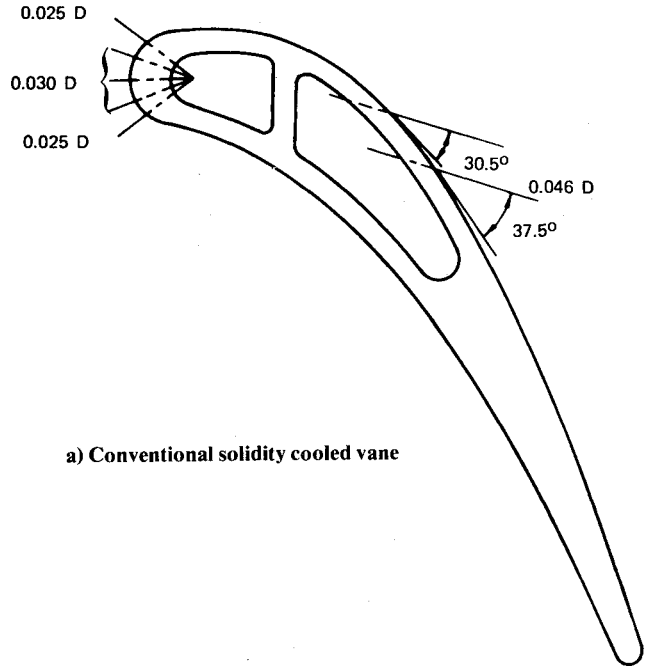
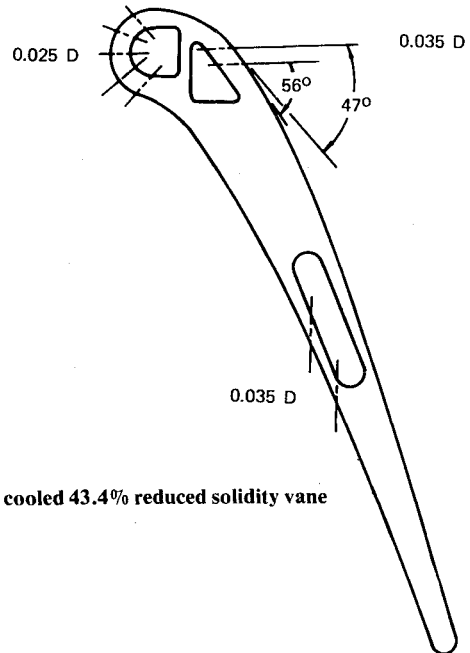


Fig. 14 Close-up of the 43.4% reduced solidity radial wafer airfoil within cascade assembly.



a) Conventional solidity cooled vane



b) First cooled 43.4% reduced solidity vane

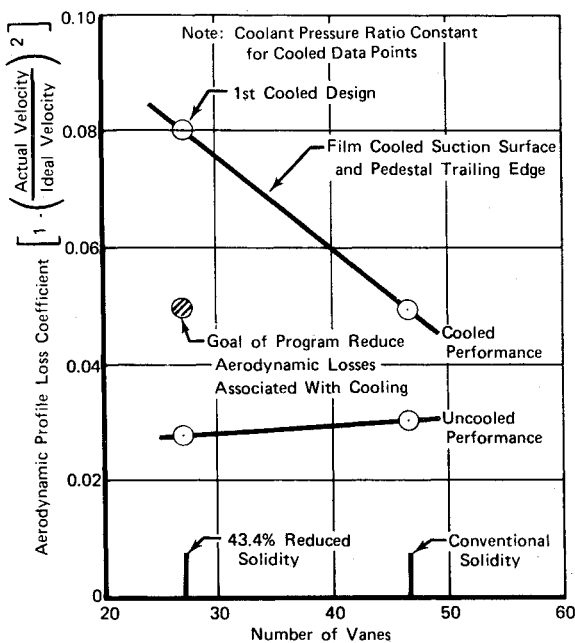


Fig. 15 Aerodynamic performance for the first-vane airfoils.

17-0.010 in. thermocouples embedded in the airfoil surface to measure wall temperature. The coolant and mainstream flowrates were determined by using ASME-calibrated orifices. The main gas stream inlet total temperature and pressure were measured by a traverse probe located at mid-span which traveled from airfoil position 2 to 6. The exit total and static pressure and the exit air angle were measured with a traverse probe located 0.2 in. downstream of the cascade. The exit probe traveled from airfoil position 2 to 6 at approximately 25% span. This location provided airfoil loss data that were not influenced either by the cascade endwall or by the thermocouple slots which ran from midspan to tip.

All data were recorded on an automatic data recording system. Manually recorded data were obtained for the critical parameters also. Exit probe traverse and recording rates were selected to assure sufficient response time for servobalance systems to accurately measure parameters, such as air angles and total pressures. All transducers measuring transients were close-coupled to the sensor. Transducers used to measure critical parameters, such as cascade total pressures loss, were selected to have accuracies of $\pm 0.2\%$ of full-scale range. The smallest transducer ranges compatible with expected pressure levels were selected.

Fig. 16 Cooling configurations for the first-vane airfoils.

Cascade Airfoil Test Results

Aerodynamic Performance

The inlet total pressure and the exit total and static pressure across the cascade were obtained from the inlet and exit traverse probes, respectively, and presented as the aerodynamic loss coefficient $(1 - \phi^2)$. (See the Appendix for description of terms and methods of data analysis.) Aerodynamic performance presented in this paper does not take into account the ideal energy or the coolant flows involved. However, this effect was negated for the various designs investigated by presenting only the data obtained at the engine design coolant pressure ratio.

Figure 15 shows the uncooled and cooled aerodynamic performance of the conventional and the first cooled 43.4% reduced solidity airfoils measured in the plane cascade rig. Uncooled aerodynamic performance of the reduced solidity airfoil compared favorably with that of the conventional

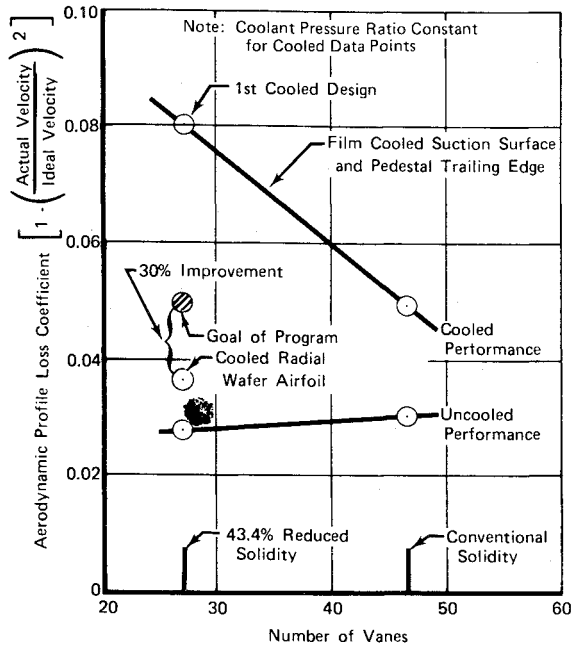


Fig. 17 Aerodynamic performance for first-vane airfoils.

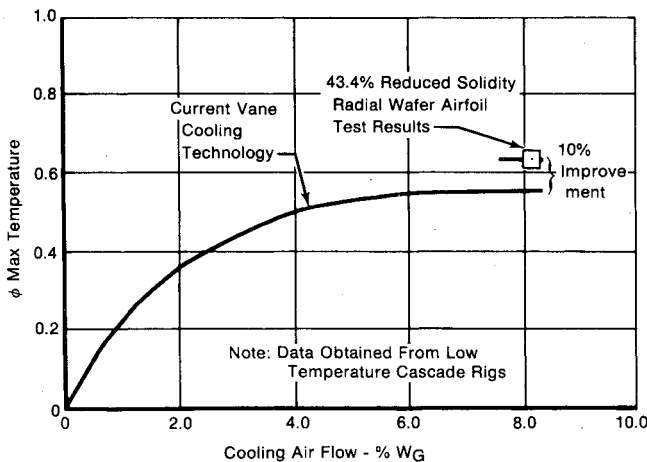


Fig. 18 Vane cooling effectiveness.

airfoil; however, the aerodynamic loss of the first-cooled 43.4% reduced solidity airfoil was much higher. The primary cause for the increase in loss was the location of the suction-side film cooling in a region of high-surface Mach number. The cooling geometries for the two designs, both having suction-side film cooling, are shown in Fig. 16. As stated in the Introduction, conventional trailing-edge cooling schemes must be augmented with film cooling for advanced reduced solidity turbines. Suction-side separation was a major concern with the reduced solidity design, so it was decided that film cooling would not be used in an area of an adverse pressure gradient because it may induce separation. Since an adverse pressure gradient exists on the suction side from the minimum pressure point to the trailing edge, the position of the film-cooled holes for the reduced solidity vane was selected as far upstream of the minimum pressure point as possible without interfering with the leading edge showerhead holes.

Cooling Performance

Although the cascade rig conditions did not simulate the engine Reynolds number or temperature ratio, it did simulate the engine Mach number and coolant pressure ratio. The cooling data reflect the cooling characteristics of the design and indicate the same cooling trends in the trailing-edge section as obtained in a separate trailing edge cooling study.¹

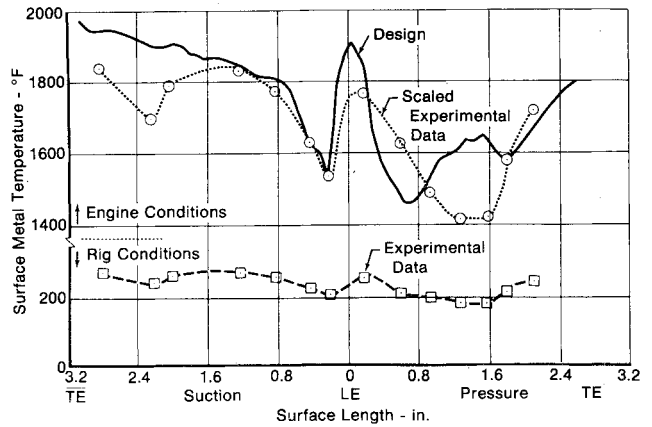


Fig. 19 Temperature profile for the 43.4% reduced solidity radial wafer airfoil, wavy crisscross slot design.

A 10% improvement in cooling effectiveness, based on the hot-spot metal temperature, was obtained with the radial wafer airfoil when compared to current vane data, as illustrated in Fig. 18. A plot of the wall temperature profile for the test airfoil at the cascade rig test conditions is shown in Fig. 19. Also included on the figure are the scaled-up metal temperatures and the final design prediction. As shown by the figure, the agreement between the predicted and experimental data is good. In the suction-side trailing edge section, the wavy crisscross design was actually more efficient than expected, and the measured wall temperatures are approximately 100°F cooler than predicted. In the region of the suction-side convective holes, the experimental data agreed well with the prediction.

V. Conclusions

Use of an efficient convective cooling scheme on the suction-side and the trailing-edge region of an advanced first-vane airfoil eliminated the need for film cooling in those regions.

Elimination of the suction-side film cooling resulted in an airfoil design with a reduction in the aerodynamic loss of approximately 30% less than the design goal which was set equal to that obtained with the cooled conventional solidity airfoil.

An effective convective cooling scheme was possible through the use of the radial wafer fabrication techniques which permit designs with small intricate convective passages not attainable in cast and drilled airfoils.

The wavy crisscross trailing-edge design required a relatively high-pressure ratio, which makes it primarily suited for the latter rows of a two-stage turbine or the first row of a single-stage turbine. The cooling design is also compatible with either the radial wafer or two-piece airfoil fabrication technique.

Appendix: Method of Data Analysis

Aerodynamic Performance

Airfoil aerodynamic efficiency η is the ratio of the actual kinetic energy leaving the nozzle, $V_a^2/2g$, to the kinetic energy for an isentropic process from the same initial conditions, $V_i^2/2g$. In other words, it is defined as the ratio of the actual to ideal enthalpy drop as illustrated in Fig. A1. The aerodynamic performance is usually expressed as the profile loss coefficient $(1-\phi^2)$, which is defined as unity minus efficiency. The profile loss coefficient may also be expressed in terms of upstream total pressure and downstream total and static pressure by

$$1 - \phi^2 = \frac{1 - (P_{o1}/P_{o2})^{(\gamma-1)/\gamma}}{1 - (P_{o1}/P_{s2})^{(\gamma-1)/\gamma}}$$

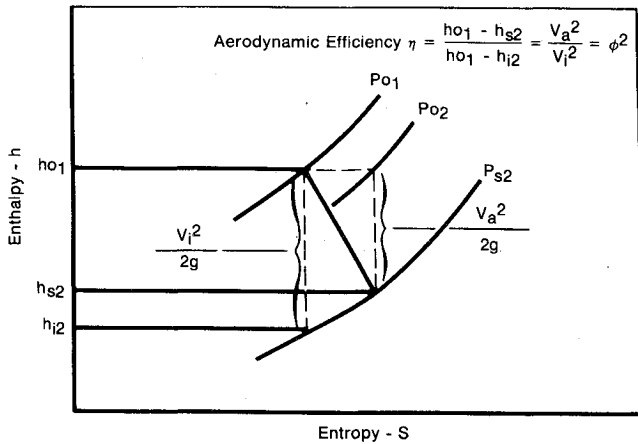


Fig. A1 Definition of airfoil aerodynamic efficiency.

Cooling Performance

The cooling performance is determined by measuring the airfoil wall temperatures at the design mainstream and coolant conditions. The cascade test was conducted at reduced temperature and pressure to reduce the complexity and cost of testing. The engine Reynolds number, Mach number, and mainstream-to-coolant temperature ratio are duplicated at the reduced cascade test conditions for ideal heat transfer simulations. Testing at the reduced temperature, however, necessitates scaling-up of the wall temperatures to engine conditions to compare the data to the design prediction. The scaling is accomplished by using the cascade rig cooling ef-

fectiveness parameters ϕ defined as

$$\phi = (T_G - T_W) / (T_G - T_C)$$

and replacing the gas stream and coolant temperature with their corresponding engine design values and solving for the engine wall temperature. This scaling procedure has been verified by comparing our reduced temperature rig results with results of high-temperature cascade tests,² as well as by NASA.³

The average and hot-spot cooling effectiveness parameters are defined as just mentioned; only T_W is replaced by the average wall temperature and the maximum wall temperature, respectively. The two effectiveness parameters are then used to compare the cooling efficiency of various cooling schemes to one another.

Acknowledgment

The work reported herein was conducted by Pratt & Whitney Aircraft Group, Government Products Division, with the support of the Air Force Aero Propulsion Laboratory, Air Force Systems Command, Wright-Patterson AFB, Ohio, under Contract F33615-76-C-2009.

References

- ¹1976 Independent Research and Development Program, Pratt & Whitney Aircraft Group, FP 76-273, Dec. 1976.
- ²1973 Independent Research and Development Program, Pratt & Whitney Aircraft, FP 72-104, Nov. 1972.
- ³Gladden, H.J. and Livingood, J.N.B., "Procedure for Scaling of Experimental Vane Airfoil Temperature From Low to High Gas Temperature," NASA TND-6510, Sept. 1971.

From the AIAA Progress in Astronautics and Aeronautics Series...

EXPERIMENTAL DIAGNOSTICS IN GAS PHASE COMBUSTION SYSTEMS—v. 53

Editor: Ben T. Zinn; Associate Editors: Craig T. Bowman, Daniel L. Hartley, Edward W. Price, and James F. Skifstad

Our scientific understanding of combustion systems has progressed in the past only as rapidly as penetrating experimental techniques were discovered to clarify the details of the elemental processes of such systems. Prior to 1950, existing understanding about the nature of flame and combustion systems centered in the field of chemical kinetics and thermodynamics. This situation is not surprising since the relatively advanced states of these areas could be directly related to earlier developments by chemists in experimental chemical kinetics. However, modern problems in combustion are not simple ones, and they involve much more than chemistry. The important problems of today often involve nonsteady phenomena, diffusional processes among initially unmixed reactants, and heterogeneous solid-liquid-gas reactions. To clarify the innermost details of such complex systems required the development of new experimental tools. Advances in the development of novel methods have been made steadily during the twenty-five years since 1950, based in large measure on fortuitous advances in the physical sciences occurring at the same time. The diagnostic methods described in this volume—and the methods to be presented in a second volume on combustion experimentation now in preparation—were largely undeveloped a decade ago. These powerful methods make possible a far deeper understanding of the complex processes of combustion than we had thought possible only a short time ago. This book has been planned as a means of disseminating to a wide audience of research and development engineers the techniques that had heretofore been known mainly to specialists.

671 pp., 6x9, illus., \$20.00 Member \$37.00 List

TO ORDER WRITE: Publications Dept., AIAA, 1290 Avenue of the Americas, New York, N.Y. 10019